



SAKARYA ÜNİVERSİTESİ

# FEN BİLİMLERİ ENSTİTÜSÜ DERGİSİ

Sakarya University Journal of Science  
SAUJS

e-ISSN 2147-835X | Period Bimonthly | Founded: 1997 | Publisher Sakarya University |  
<http://www.saujs.sakarya.edu.tr/en/>

Title: The Effect of Hydrothermal Aging Time and Temperature on the Structural Properties of KIT-6 Material

Authors: Dilşad Dolunay ESLEK KOYUNCU

Received: 2020-06-19 20:25:30

Accepted: 2021-01-05 12:55:21

Article Type: Research Article

Volume: 25

Issue: 1

Month: February

Year: 2021

Pages: 240-251

How to cite

Dilşad Dolunay ESLEK KOYUNCU; (2021), The Effect of Hydrothermal Aging Time and Temperature on the Structural Properties of KIT-6 Material. Sakarya University

Journal of Science, 25(1), 240-251, DOI:

<https://doi.org/10.16984/saufenbilder.755286>

Access link

<http://www.saujs.sakarya.edu.tr/en/pub/issue/58068/755286>

New submission to SAUJS

<https://dergipark.org.tr/en/journal/1115/submission/step/manuscript/new>

## The Effect of Hydrothermal Aging Time and Temperature on the Structural Properties of KIT-6 Material

Dilşad Dolunay ESLEK KOYUNCU \*<sup>1</sup>

### Abstract

The combined effect of hydrothermal treatment temperature and aging time on the structural properties of ordered mesoporous KIT-6 material were investigated. A series of KIT-6 materials were prepared by hydrothermal synthesis procedure. In the first step, experiments were performed at 90°C and at different aging times (0-72 h) to understand the effect of hydrothermal aging time. It was concluded that the aging time positively affect the formation of ordered mesoporous structure and uniform pore structure occurs after 18 h. In addition, long hydrothermal treatment time favored the pore enlargement. In the second step, to understand which parameter (time or temperature) is more important in the synthesis of highly uniform material, KIT-6 materials were prepared at different temperatures ranging between 60-150°C and at different aging times (24 h and 72 h). The experiments showed that at elevated temperatures (>90°C) long aging times negatively affect the structural properties of the mesoporous KIT-6 structure. Highly uniform mesoporous KIT-6 material having high crystallinity, narrow pore size distribution, high BET surface area (726 cm<sup>3</sup>/g) and high pore volume (1.5 cm<sup>3</sup>/g) was prepared at 120°C with an aging time of 24 h. However, it was determined that 60°C is not a suitable temperature to obtain KIT-6 material having good structural properties and the uniform crystal structure deteriorated at 150°C.

**Keywords:** KIT-6, Mesoporous silica, Aging time, Hydrothermal synthesis, Temperature effect

### 1. INTRODUCTION

Porous materials are divided into three basic groups in terms of their pore sizes according to IUPAC (International Union of Pure and Applied Chemistry) classification. In this context, the materials having pores widths larger than 50 nm are called macroporous; those with pores widths between 2 nm and 50 nm are called mesoporous

and those with pores widths smaller than 2 nm are called microporous [1]. Mesoporous materials with superior properties have attracted great attention due to their potential use in many areas since M41S family was firstly reported by Mobil Oil Corporation [2]. MCM-41, MCM-48 and MCM-50 which are the most well-known materials of this class are ordered in hexagonal (space group p6mm), cubic (space group Ia3d)

\* Corresponding Author: [deslek@gazi.edu.tr](mailto:deslek@gazi.edu.tr)

<sup>1</sup> Gazi University, ORCID: <https://orcid.org/0000-0001-8092-6740>

and lamellar (space group  $p2$ ) arrays, respectively [3]. These mesoporous materials have high surface areas (higher than  $700 \text{ m}^2/\text{g}$ ), pore volume (greater than  $1.7 \text{ cm}^3/\text{g}$ ) and ordered framework [4]. In 1998, Zhao et al. (1998) prepared the highly ordered mesoporous SBA (Santa Barbara Amorphous) family under acidic conditions using non-ionic surfactant as a directing agent [5]. SBA-15 is one of the most important material of this family. SBA-15 is synthesized in an acidic medium using the non-ionic triblock copolymer Pluronic P123 as a surfactant. Similar to the MCM-41 structure, SBA-15 has a hexagonal structure with a spatial group of  $p6mm$ . However, it shows greater hydrothermal stability although it has thicker silica walls (3.1 to 6.4 nm) and larger pores (4.6 to 30 nm) than MCM-41 material [6].

KIT-6 material, which is a cubic  $Ia3d$  form of mesoporous silica, firstly synthesized by Korea Advanced Institute of Science and Technology (KAIST). Similar to MCM-48 structure, it has interpenetrating bi-continuous pore system with three dimensional cubic  $Ia3d$  symmetric structure but with larger pore diameter [7-8]. Bi-continuous channel structure of KIT-6 materials provides more active area and resistance to agglomeration [9]. In addition, the tunable pore size of this material makes the material more advantageous in terms of active metal dispersion and reactant accessibility especially in catalytic applications. By changing the synthesis conditions, such as hydrothermal treatment temperature, surfactant

type and surfactant concentration, the pore size of KIT-6 material can be tuned from 4 to 12 nm [8,10]. In the literature, KIT-6 materials have been studied for various applications as adsorbent [11], catalyst support [12,13], nano-casting template for the synthesis of Si-free mesoporous materials, such as carbon [14],  $\text{TiO}_2$  [15],  $\text{C}_3\text{N}_4$  [16],  $\alpha\text{-Fe}_2\text{O}_3$  [17], Au [18],  $\text{MnO}_2$  [19],  $\text{RuO}_2$  [20]. The most important reason of using KIT-6 material as a support material is the unique 3D interpenetrating pore structure which allows direct and open access of guest molecules without pore blocking [7,21,22]. In the literature, KIT-6 is used as support material in the dehydrogenation of propane [23,24],  $\text{CO}_2$  removal [25],  $\text{CO}_2$  reforming of methane [26], methane production via hydrogenation of  $\text{CO}_2$  [27], hydrogenation of CO [28] etc.

Figure 1 shows the typical hydrothermal synthesis of KIT-6 material. The hydrothermal method was reported as a very important method as it enables high quality crystal formation [29]. The synthesis is performed in acidic medium of HCl. Triblock co-polymer P123 (PEO-PPO-PEO) and tetraethyl orthosilicate (TEOS) are used as surfactant and silica source, respectively. Different from the synthesis of SBA-15 material, butanol is added as co-solvent and co-surfactant [30]. It has been reported that butanol provides phase transformation and low amounts of butanol (butanol / P123 < 0.9 by weight) cause the formation of 2D hexagonal mesophase [10].

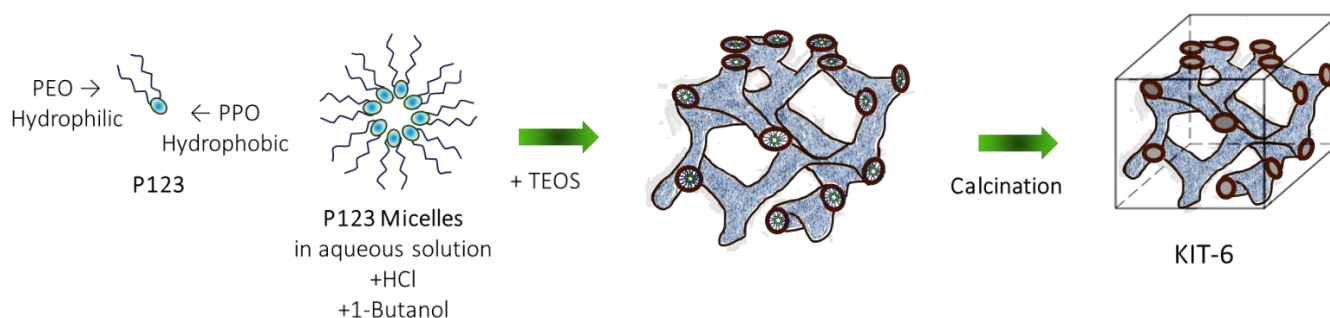


Figure 1. Typical hydrothermal synthesis mechanism of KIT-6 material

In this study, the effect of hydrothermal treatment parameters on the structural properties of mesoporous KIT-6 materials was investigated. A

series of KIT-6 materials were prepared by hydrothermal synthesis procedure. In the first step, the effect of hydrothermal treatment

duration on the structural properties of KIT-6 materials was studied at hydrothermal treatment temperature of 90°C. In the second step, to understand which parameter (time or temperature) is more important in the synthesis of highly uniform material, KIT-6 materials were prepared at different temperatures ranging between 60-150°C and at selected aging times at which the mesopore structure can be obtained. Structural changes in the KIT-6 materials were determined by characterization studies. There is no study present in the literature that investigate the combined effect of hydrothermal treatment duration and temperature on the structural properties of mesoporous KIT-6 material.

## 2. MATERIAL AND METHOD

### 2.1. Synthesis of Mesoporous KIT-6 Material

In this study, a series of KIT-6 materials were prepared by hydrothermal synthesis procedure as reported in the literature [31]. Firstly, until reaching complete dissolution 6 g of surfactant, Triblock copolymer Pluronic P123 (poly(ethylene oxide) - poly(propylene oxide) - poly(ethylene oxide), Sigma-Aldrich, molecular weight $\approx$ 5800), 220 ml of deionized water and 12 g of co-solvent concentrated HCl (Sigma-Aldrich, 37%) were stirred at 35°C. Then, 6 g of co-surfactant 1-Butanol (Alfa Aesar, 99 %) was added to this mixture. After 1 hour mixing at the same temperature, 12.4 g of Tetraethyl orthosilicate, TEOS (Sigma-Aldrich, 98%), was added as silica source. Mixing was carried out for 24 hours at the same temperature. The resulting mixture was transferred into a Teflon lined autoclave and hydrothermal treatment was performed under static conditions at different times (h=0-12-18-24-48-72 hours) and at different temperatures (t=60-90-120-150°C). The solid product was recovered by vacuum filtration and washed with deionized water several times until the pH of the filtrate remained constant. The solids were oven dried at 90°C and calcined at 750°C for 6 hours with a heating rate of 10°C/min in air flow. The materials obtained via this procedure were named as KITt-h, where “t” stands for hydrothermal

treatment temperature and “h” represents the duration of the hydrothermal treatment.

### 2.2. Characterization Studies

Crystalline phases of the KIT-6 samples were determined by the low-angle powder X-ray diffraction (XRD) analysis, using a Rigaku Ultima-IV diffractometer with Cu K $\alpha$  radiation (40 kV and 30 mA) at a scanning rate of 0.2°min<sup>-1</sup>. The N<sub>2</sub> adsorption/desorption isotherms were obtained with Quantachrome Autosorb-1C model equipment, at 77 K and the samples were vacuum dried at 250°C for 3 h before the experiments. The specific surface areas of KIT-6 samples were calculated using the desorption points within the N<sub>2</sub> relative pressure range of 0.05-0.30 using Brunauer-Emmett-Teller (BET) method. The pore size distributions of the samples were obtained from the analysis of the desorption values by using the Barrett-Joyner-Halenda (BJH) method. The functional groups present in the structure were investigated by Fourier-Transform Infrared spectroscopy (FT-IR) in the medium infrared region of 4000-400 cm<sup>-1</sup> with 4 cm<sup>-1</sup> resolutions in a Jasco 4700 ATR/FT-IR spectrophotometer.

## 3. RESULTS AND DISCUSSION

A series of KIT-6 materials were prepared via hydrothermal synthesis procedure. At the first stage, the aging time of hydrothermal treatment was varied from 12 h to 72 h at 90°C to determine the effect of aging time on the structural properties of the resulting materials. A material without hydrothermal treatment was also prepared for the comparison. The 3D ordered mesoporous silica structure were determined by the small angle XRD patterns of the KIT-6 materials (Figure 2). As it is seen in Figure 2 that the aging time has crucial effect on the crystal structure of the final material. The peak intensity of the KIT90-24 sample is larger than other prepared materials. This might be resulted from the highly organized framework with uniformly packed silica crystals. The KIT90-24 sample exhibited three characteristic XRD peaks at 2 $\theta$ =1.06°, 1.2° and 1.9°, corresponding to (211),

(220) and (332) Miller indices that are the characteristics of three-dimensional mesoporous structures with spatial group Ia3d organized in body-centered cubic array [32]. As the aging time increases to 72 h the XRD peak intensity decreases to the lower values (KIT90-72). This may be the indication of deterioration in uniform crystal structure of the KIT90-72 sample because of high aging duration. In the XRD patterns of KIT90-12 and KIT90-18 samples, only the main peak of KIT-6 structure was observed with lower intensity. In the XRD patterns of the KIT-0 sample prepared without hydrothermal treatment, no peak observed that is the indication of any crystal structure.

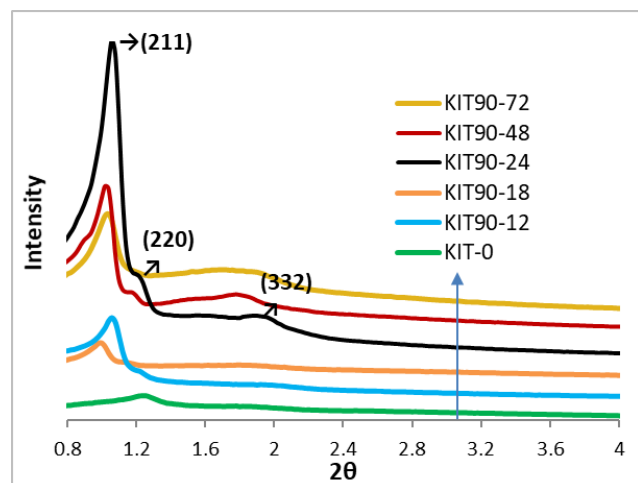


Figure 2. Small angle XRD patterns of KIT-6 materials prepared at 90°C

The interplanar spacing ( $d_{211}$ ), the lattice parameter ( $a_0$ ) and the wall thickness ( $t$ ) values were calculated for all samples (Table 1). The interplanar spacing, which is the periodic interval of pores of KIT-6 that is the summation of the pore width and the pore wall, was calculated from Bragg's Law ( $n\lambda=2d \sin\theta$ ) by using the  $2\theta$  value of the (211) peak. It was observed that the wall thickness decreases slightly from 4.8 nm to 4.0 nm with the increasing aging time. Similar results were observed in the study of Merkache et al. (2015). They compared the structural changes of KIT-6 materials prepared at 100°C with aging times of 48 h and 72 h. They have reported that

the wall thickness decreases from 4.07 nm to 3.77 nm with aging time [33].

The bands related to the inorganic functional groups of KIT-6 structure were observed in the ATR/FT-IR spectra (Figure 3). It is seen that the peak intensity increases as the aging time increases. It might be due to the higher degree of TEOS silanization at longer aging times. It is known that the main bands around  $1034 \text{ cm}^{-1}$ ,  $800 \text{ cm}^{-1}$  and  $445 \text{ cm}^{-1}$  are related with the structural siloxane (Si-O-Si) framework. The band at  $1034 \text{ cm}^{-1}$  and identified shoulder at  $1204 \text{ cm}^{-1}$  are the typical bands referring to asymmetric stretching of the Si-O-Si bond [33]. Bands around  $810 \text{ cm}^{-1}$  and  $445 \text{ cm}^{-1}$  could be attributed to symmetrical stretching and bending vibrations of the Si-O-Si bond, respectively [34]. A small broad peak at about  $\sim 3400 \text{ cm}^{-1}$  are assigned to the stretching of OH groups of water adsorbed to the surface. Small vibrations between  $1900\text{-}2400 \text{ cm}^{-1}$  are the characteristics of ATR measurements.

The  $\text{N}_2$  adsorption-desorption isotherms of the KIT-6 materials prepared at 90°C in different aging times are classified as Type IV according to the IUPAC classification (Figure 4). A sharp capillary condensation step at high relative pressures (nearly at  $P/P^0=0.6\text{-}0.8$ ) and a final saturation plateau are the characteristics of this type of isotherms [30]. It is known that there is a correlation between the shape of observed hysteresis loop and the textural properties of the material [35]. All samples exhibit hysteresis loop at pressure ranges of  $P/P^0=0.5\text{-}0.8$ . The narrow hysteresis loop is the indication of the highly uniform pore structure. As it is seen that the regular pore structure occurs after 18 hours aging time. Non-uniform  $\text{N}_2$  adsorption-desorption isotherm was obtained with the KIT-0 sample prepared without hydrothermal treatment. According to the IUPAC classification the samples exhibited the H1 type hysteresis loop that is related with the well-ordered three-dimensional mesopore networks of KIT-6 material [35,36]. After 24 hours of aging, adsorbed volume is decreased with increasing aging time.

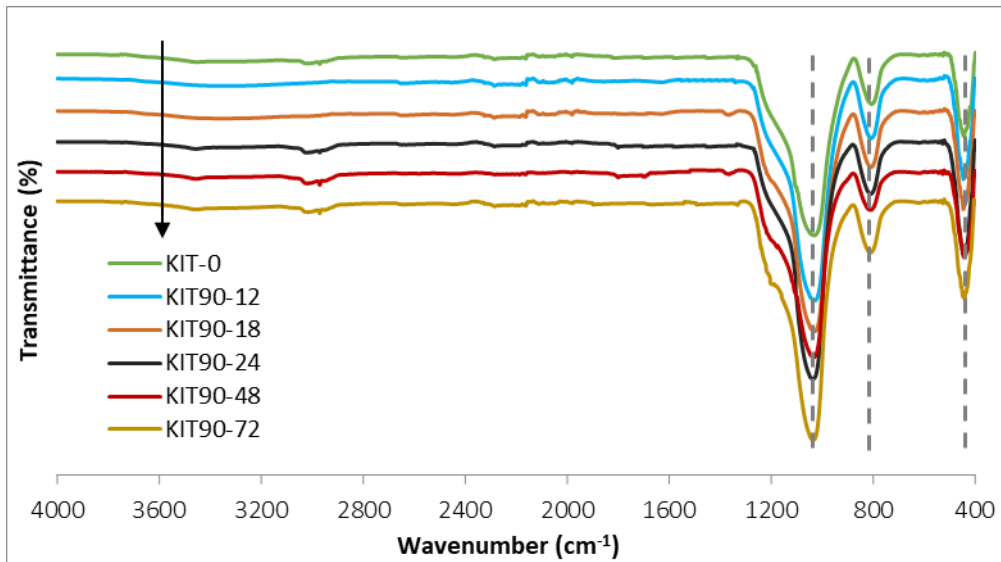
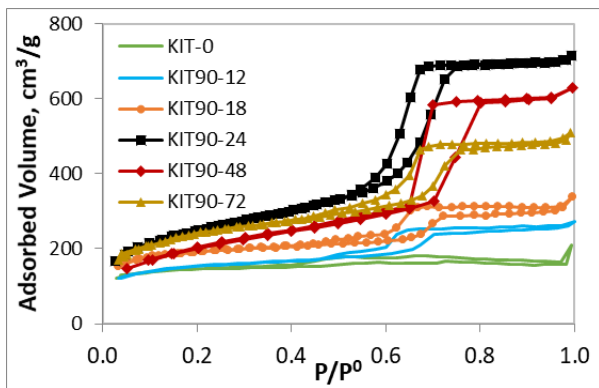


Figure 3. ATR/FT-IR spectrum of KIT-6 materials prepared at 90°C

Figure 4. N<sub>2</sub> adsorption-desorption isotherms of KIT-6 materials prepared at 90°C

The pore size distribution curves determined by BJH method are given in Figure 5. KIT90-24 and KIT90-48 samples were exhibited mono-disperse pore size distribution. The pore size distribution curve of the KIT-0 sample is also given as an inner figure as a comparison. The importance of the hydrothermal treatment in the formation of mesopore structure can be seen in this graph.

Table 1 summarizes the XRD and BET results of KIT90 materials. The interplanar spacing ( $d_{211}$ ), lattice parameter ( $a_0$ ) and wall thickness ( $t$ ) values were calculated for all samples. The interplanar spacing is the periodic interval of pores of KIT-6 that is the summation of the pore width and the pore wall. This value was calculated from Bragg's Law ( $n\lambda=2d \sin\theta$ ) by using the  $2\theta$  value of the (211) peak of the samples. While there is no important change in the  $d_{211}$  and  $a_0$  values, the

pore diameter slightly increases with aging time. Thus, the wall thickness of the materials decreases from 4.8 nm to 4.0 nm as the aging time increases from 12 h to 72 h. This indicates that long hydrothermal treatment duration favors the pore enlargement. Similar results were obtained by Fernandes et al. (2018). They have reported that when the aging time increases from 12 h to 30 h, the pore diameter increases from 6.1 nm to 7.0 nm, respectively [30]. The KIT90-24 sample exhibited the highest BET surface area and pore volume compared to the other prepared KIT-6 supported materials.

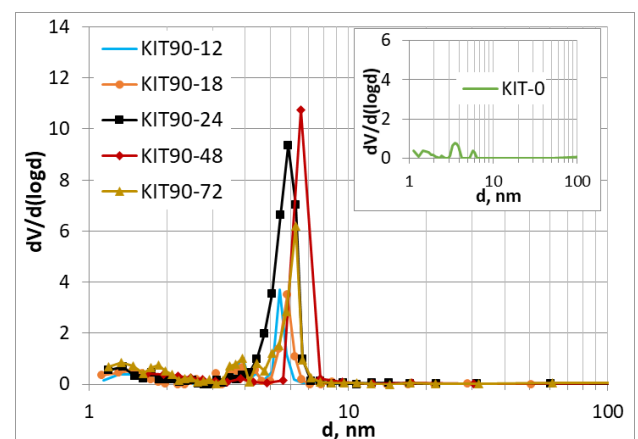


Figure 5. Pore size distribution curves of KIT-6 materials prepared at 90°C

Table 1. XRD and N<sub>2</sub> adsorption-desorption results at different aging times of materials prepared at 90°C

Sample	Aging temperature °C	Aging time hour	d <sub>211</sub> <sup>a</sup> nm	a <sub>0</sub> <sup>b</sup> nm	Wall thickness <sup>c</sup> t, nm	Pore diameter <sup>d</sup> d <sub>p</sub> , nm	Pore volume <sup>d</sup> V <sub>p</sub> , cm <sup>3</sup> /g	BET surface area <sup>d</sup> m <sup>2</sup> /g
KIT90-0	-	0	-	-	-	1.1	0.24	470
KIT90-12	90	12	8.33	20.4	4.8	5.4	0.35	497
KIT90-18		18	8.83	21.6	5.0	5.8	0.43	615
KIT90-24		24	8.33	20.4	4.3	5.9	1.12	858
KIT90-48		48	8.65	21.2	4.1	6.5	0.93	670
KIT90-72		72	8.35	20.8	4.0	6.2	0.76	796

<sup>a</sup> Interplanar spacing calculated from Bragg's Law

<sup>b</sup> Cubic parameter,  $a_0 = d_{211} \cdot \sqrt{h^2 + l^2 + k^2}$

<sup>c</sup>  $t = a_0/2 - d_p$

<sup>d</sup> Obtained from BJH desorption data

In the next stage of the study, experiments were carried out at different temperatures (60-150°C) and aging times (24 h and 72 h) to understand which parameter is more important in the synthesis of highly uniform KIT-6 materials. Aging times of 24 h and 72 h were selected at this stage. Because it is concluded in the previous stage that in the studied aging time range these treatment times are the lowest and highest temperatures at which the uniform mesoporous structure is obtained.

The XRD patterns of materials that are hydrothermally treated at different temperatures for 24 h and 72 h are given in Figure 6. Materials other than KIT120-72 and KIT150-24 exhibited all characteristic XRD peaks of mesoporous KIT-6 crystal structure. The peak intensity of the materials differs with respect to the aging temperature and aging time of the synthesis. With aging time of 24 h, it is seen that the peak intensity increases and the peaks shift to the left side with increasing temperature from 60 °C to 120°C. This results the increase in the interplanar spacing and the cubic parameter. When the temperature was raised to 150°C, the XRD peak became smaller and the other characteristic peaks of KIT-6 structure disappeared except for the main peak. This can be attributed to the deterioration of uniform crystal structure. However, in the XRD patterns of the materials with aging time of 72 h, when the temperature was increased from 60°C to 90°C the peak intensity decreases sharply and shifted to the left side. The KIT-6 material was also prepared at 150°C with an aging time of 72 h and it was observed that the material deteriorated (its result not shown in Figure). It can be concluded from these results that especially at higher temperatures long aging time causes to the

deformation of regular crystal structure of KIT-6 material.

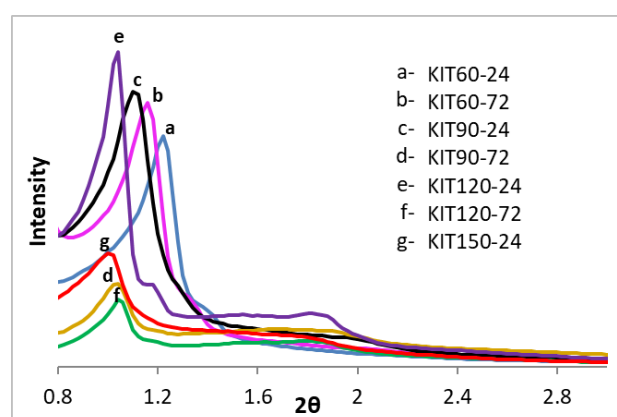


Figure 6. XRD patterns of KIT-6 materials prepared at different temperatures and at different aging times

The ATR/FT-IR spectra of KIT-6 materials prepared at different temperatures and at different aging times are given in Figure 7. As mentioned earlier, the band at 1050 cm<sup>-1</sup> and identified shoulder at about 1204 cm<sup>-1</sup> are the typical bands referring to asymmetric stretching of the Si-O-Si bond [33]. Bands around 800 cm<sup>-1</sup> and 445 cm<sup>-1</sup> could be attributed to symmetrical stretching and bending vibrations of the Si-O-Si bond, respectively [34]. It is clearly observed in the FT-IR results that peak intensities become higher when the temperature raised from 60°C to 150°C. It might be due to the higher degree of TEOS silanization at higher temperatures [37]. The hydrolysis of TEOS is the first step in the preparation of mesoporous silica materials using TEOS as a silica source. [38]. The efficiency of the hydrolysis process affects the properties of the final material. In addition to the water amount, temperature is very important parameter affecting the hydrolysis reaction efficiency. As long as water amount is sufficient and temperature is

high, TEOS is completely hydrolyzed and much Si-O-Si bond was gained. Because of the endothermic nature of the hydrolysis process high temperatures favor the formation of Si-O-Si bond [39]. The reason for getting high density FT-IR peaks at high temperatures can be explained in this way.

The N<sub>2</sub> adsorption-desorption isotherms of the KIT-6 samples prepared at different aging temperatures and aging times are classified as Type IV (Figure 8). It can be seen in the Figure 8

that all samples exhibit hysteresis loop at pressure ranges of  $P/P^0=0.5-0.8$ . The H1 type hysteresis loop of the samples is related with the well-ordered three-dimensional mesopore networks of KIT-6 material [35,36]. When the aging time increased from 24 hours to 72 hours, there was no significant change in the isotherm and hysteresis patterns of the samples. However, it is noteworthy that there is some shift in the isotherm and changes in the pore properties such as; pore diameter, pore volume, BET surface area, etc.

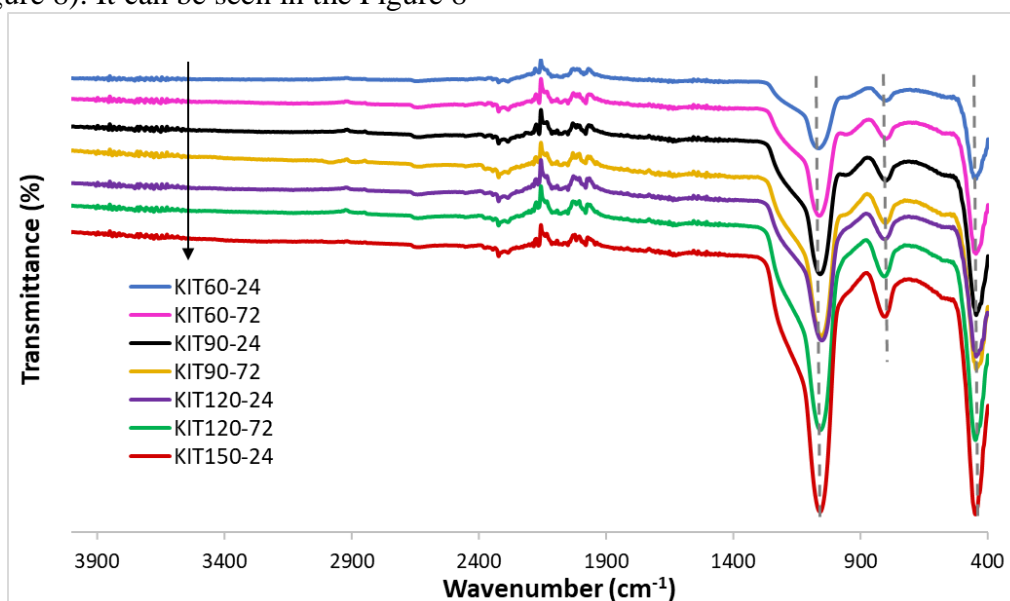


Figure 7. ATR/FT-IR spectrum of KIT-6 materials prepared at different hydrothermal treatment temperatures and at different aging times

If the temperature effect is compared for the same aging times, it is seen that at lower temperatures (especially at 60°C), the hysteresis loop shifted to the left side and the adsorbed volume decreased. The pore diameter (4.2 nm), pore volume (0.67 cm<sup>3</sup>/g) and BET surface area (665 m<sup>2</sup>/g) values of this sample (KIT60-24) were found to be lowest at the end of 24 h aging as compared with the other studied samples (Table 2).

It was concluded that 60°C temperature is not sufficient to obtain KIT-6 material having good mesopore structure. When the temperature raised to the 120°C, the hysteresis loop shifts to the right side and become narrower. This is the indication of the highly uniform pore structure. Interestingly, in the example of KIT150-24, it has been determined that the cubic parameter, pore volume and pore diameter are significantly increased, therefore the wall thickness and BET

surface area are also decreased. It was determined that this may be due to the deterioration in uniform mesopores of the materials because of the high synthesis temperature. If the aging time effect is compared at different temperatures it is seen that increasing aging time has positive effect on the structural properties up to 90°C. However, if the aging time increases from 24 h to 72 h at higher temperatures (>90°C), the pore size distribution becomes broader (Figure 9), pore volume and pore diameter increases thus the wall thickness and BET surface area decreases. It has been determined from these results that at elevated temperatures (120°C) long aging times negatively affect the structural properties of the mesoporous KIT-6 structure.

To determine the morphological changes in the samples, SEM analysis were performed for

KIT90-24 and KIT120-24 samples (Figure 10). Although there is not much difference between 90 °C and 120 °C, it is seen that there is a significant change in the morphological structure. As the hydrothermal temperature increased to 120 °C, the rigid structure of the KIT-6 transformed into a flower-like structure with smaller particles. From the SEM images, it can be evaluated that the KIT120-24 sample has a higher pore volume and pore diameter. These results were also supported by N<sub>2</sub> adsorption-desorption analysis (Table 2).

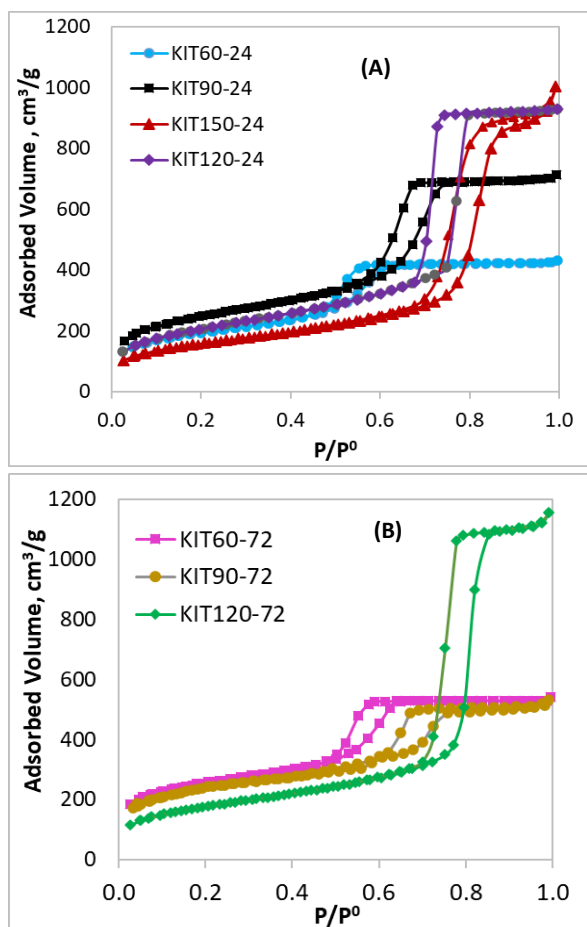


Figure 8. N<sub>2</sub> adsorption-desorption isotherms of KIT-6 materials prepared at different temperatures and at different aging times (A) 24 h (B) 72 h

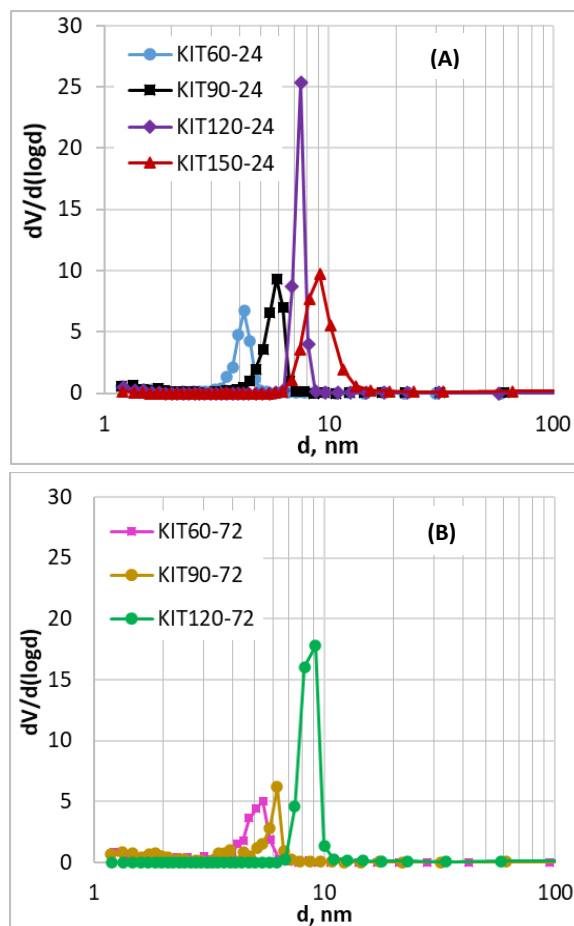


Figure 9. The pore size distribution of KIT-6 materials prepared at different temperatures and at different aging times (A) 24 h (B) 72 h

At the end of characterization results, KIT120-24 material was determined as a suitable support material having narrow pore size distribution, high BET surface area (726 cm<sup>3</sup>/g) and high pore volume (1.5 cm<sup>3</sup>/g) among the other prepared samples. Results showed that this material can be used efficiently as sorbent material in many gas/liquid adsorption studies and catalyst support material in the heterogenous reaction processes.

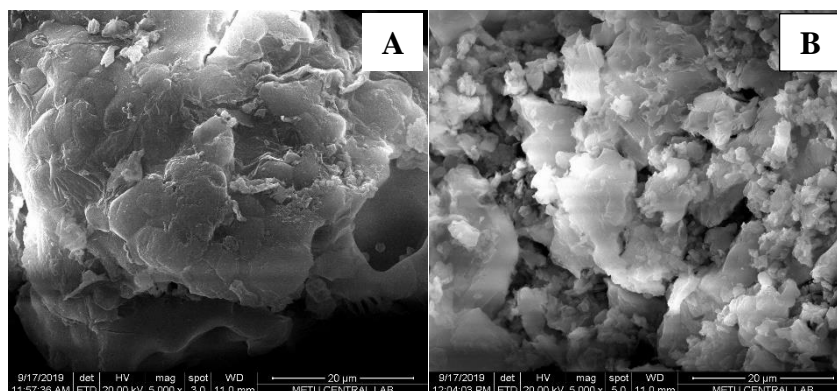


Figure 10. SEM images of (A) KIT90-24 and (B) KIT120-24 samples (x 5000)

Table 2. XRD and BET results of KIT-6 materials prepared at different hydrothermal treatment temperatures and at different aging times

Sample	Aging temperature °C	Aging time hour	$d_{211}^a$ nm	$a_0^b$ nm	Wall thickness <sup>c</sup> t, nm	Pore diameter <sup>d</sup> $d_p$ , nm	Pore volume <sup>d</sup> $V_p$ , cm <sup>3</sup> /g	BET surface area <sup>d</sup> m <sup>2</sup> /g
KIT60-24	60	24	7.24	17.7	4.7	4.2	0.67	665
KIT90-24	90		7.88	19.3	3.8	5.9	1.12	858
KIT120-24	120		8.49	20.8	2.9	7.5	1.5	726
KIT150-24	150		8.65	21.2	1.5	9.1	1.62	554
KIT60-72	60	72	7.61	18.6	4.5	4.8	0.88	817
KIT90-72	90		8.35	20.8	4.0	6.2	0.76	796
KIT120-72	120		8.49	20.8	2.2	8.2	1.97	621

<sup>a</sup> Interplanar spacing calculated from Bragg's Law

<sup>b</sup> Cubic parameter,  $a_0 = d_{211} \cdot \sqrt{h^2 + l^2 + k^2}$

<sup>c</sup>  $t = a_0/2 - d_p$

<sup>d</sup> Obtained from BJH desorption data

#### 4. CONCLUSION

In this study, the combined effects of hydrothermal treatment temperature and aging time on the structural properties of ordered mesoporous KIT-6 material were investigated. Characterization results confirmed that the temperature and aging time are the two important parameters that effect the crystal and pore structure of the material. The experiments performed at 90°C revealed that aging time positively affect the formation of ordered mesoporous structure and regular pore structure occurs after 18 hours aging time. In addition, it was concluded that long hydrothermal treatment duration favors the pore enlargement. Highly uniform mesoporous KIT-6 sample having high

crystallinity, narrow pore size distribution, high BET surface area (726 cm<sup>3</sup>/g) and high pore volume (1.5 cm<sup>3</sup>/g) was prepared at 120°C with an aging time of 24h. However, it was reported that 60°C is not a suitable temperature to obtain KIT-6 sample having good mesopore structure and the deterioration of uniform crystal structure was observed at 150°C. The experiments conducted at different aging times showed that at elevated temperatures long aging times negatively affect the structural properties of the mesoporous KIT-6 structure.

#### Acknowledgement

The author would like to thanks to the Central Laboratory of METU for the characterization results of the synthesized materials.

### **Funding**

This work was financially supported by Gazi University Research Fund (Grant No. 06/2019-02).

### **The Declaration of Conflict of Interest/ Common Interest**

No conflict of interest or common interest has been declared by the author.

### **The Declaration of Ethics Committee Approval**

The author declares that this document does not require an ethics committee approval or any special permission.

### **The Declaration of Research and Publication Ethics**

The author of the paper declare that they comply with the scientific, ethical and quotation rules of SAUJS in all processes of the paper and that they do not make any falsification on the data collected. In addition, they declare that Sakarya University Journal of Science and its editorial board have no responsibility for any ethical violations that may be encountered, and that this study has not been evaluated in any academic publication environment other than Sakarya University Journal of Science.

## **REFERENCES**

- [1] K.S.V. Sing, D.H. Everett, R.A.W. Haul, L. Moscou, R.A. Pierotti, J. Rououerol, and T. Siemieniowska, "Reporting physisorption data for gas/solid systems with special reference to the determination of surface area and porosity," *Pure & Applied Chemistry*, vol. 57, no. 4, pp. 603-619, 1985.
- [2] A.M. Basso, B.P. Nicola, K. Bernardo-Gusmao, and S.B.C. Pergher, "Tunable effect of the calcination of the silanol groups of KIT-6 and SBA-15 Mesoporous Material," *Applied Sciences*, vol. 10, pp. 970-986, 2020.
- [3] F. Hoffmann, M. Cornelius, J. Morell, and M. Froeba, "Silica-Based mesoporous organic-inorganic hybrid materials," *Angewandte Chemie International Edition*, vol. 45, pp. 3216-3251, 2006.
- [4] D.E. Boldrini, S. Angeletti, P.M. Cervellini, and D.M. Reinoso, "Valorization of natural sediment," *ACS Sustainable Chemical Engineering*, vol. 7, pp. 4684-4691, 2019.
- [5] D. Zhao, J. Feng, Q. Huo, N. Melosh, G.H. Fredrickson, B.F. Chmelka, and G.D. Stucky, "Triblock copolymer syntheses of mesoporous silica with periodic 50 to 300 angstrom pores," *Science*, vol. 279, no. 5350, pp. 548-552, 1998.
- [6] R.A. Sacramento, O.M.S. Cysneiros, B.J.B. Silva, and A.O.S. Silva, "Synthesis and characterization of mesoporous materials with SBA and MCM structure types," *Cerâmica*, vol. 65, pp. 585-591, 2019.
- [7] B. Li, X. Luo, J. Huang, X. Wang, and Z. Liang, "One-pot synthesis of ordered mesoporous Cu-KIT-6 and its improved catalytic behavior for the epoxidation of styrene: Effects of the pH value of the initial gel," *Chinese Journal of Catalysis*, vol. 38, pp. 518-528, 2017.
- [8] W. Wang, R. Qi, W. Shan, X. Wang, Q. Jia, J. Zhao, C. Zhang, and H. Ru, "Synthesis of KIT-6 type mesoporous silicas with tunable pore sizes, wall thickness and particle sizes via the partitioned cooperative self-assembly process," *Microporous and Mesoporous Materials*, vol. 194, pp. 167-173, 2014.
- [9] L. Xu, C. Wang, and J. Guan, "Preparation of acid-base bifunctional mesoporous KIT-6 (KIT: Korea Advanced Institute of Science and Technology) and its catalytic performance in Knoevenagel reaction," *Journal of Solid State Chemistry*, vol. 213, pp. 250-255, 2014.
- [10] F. Kleitz, S.H. Choi, and R. Ryoo, "Cubic Ia3d large mesoporous silica: synthesis and replication to platinum nanowires, carbon nanorods and carbon nanotubes," *The Royal Society of Chemistry*, pp. 2136-2137, 2003.
- [11] R. Kishor, and A.K. Ghoshal, "APTES grafted ordered mesoporous silica KIT-6 for CO<sub>2</sub> adsorption," *Chemical Engineering Journal*, vol. 262, pp. 882-890, 2015.
- [12] Q. Liu, J. Li, Z. Zhao, M. Gao, L. Kong, J. Liu and Y. Wei, "Design, synthesis and

- catalytic performance of vanadium-incorporated mesoporous silica KIT-6 catalysts for the oxidative dehydrogenation of propane to propylene,” *Catalysis Science & Technology*, vol. 6, pp. 5927-5941, 2016.
- [13] F. He, J. Luo, and S. Liu, “Novel metal loaded KIT-6 catalysts and their applications in the catalytic combustion of chlorobenzene,” *Chemical Engineering Journal*, vol. 294, pp. 362–370, 2016.
- [14] D. Saikia, T.H. Wang, C.J. Chou, J. Fang, L.D. Tsai and H.M. Kao, “A comparative study of ordered mesoporous carbons with different pore structures as anode materials for lithium-ion batteries,” *RSC Advances*, vol. 5, pp. 42922–42930, 2015.
- [15] H. Tang, Y. Ren, S. Wei and G. Liu, “Preparation of 3D ordered mesoporous anatase TiO<sub>2</sub> and their photocatalytic activity,” *Rare Metals*, vol. 38, pp. 453–458, 2019.
- [16] S.N. Talapaneni, K. Ramadass, S.J. Ruban, M. Benzigar, K.S. Lakhi, J.H. Yang, U. Ravon, K. Albahily and A. Vinu, “3D cubic mesoporous C<sub>3</sub>N<sub>4</sub> with tunable pore diameters derived from KIT-6 and their application in base catalyzed Knoevenagel reaction,” *Catalysis Today*, vol. 324, pp. 33–38, 2019.
- [17] M. Dutt, A. Kaushik, M. Tomar, V. Gupta and V. Singh, “Synthesis of mesoporous  $\alpha$ -Fe<sub>2</sub>O<sub>3</sub> nanostructures via nanocasting using MCM-41 and KIT-6 as hard templates for sensing volatile organic compounds (VOCs),” *Journal of Porous Materials*, vol. 27, pp. 285–294, 2020.
- [18] Y. Shimasaki, M. Kitahara, M. Shoji, A. Shimojima and H. Wada, “Preparation of ordered mesoporous Au using double gyroid mesoporous silica KIT-6 via a seed-mediated growth process,” *Chemistry, An Asian Journal*, vol. 13, no. 24, pp. 3935–3941, 2018.
- [19] B. Bai, Q. Qiao, Y. Li, Y. Peng and J. Li, “Effect of pore size in mesoporous MnO<sub>2</sub> prepared by KIT-6 aged at different temperatures on ethanol catalytic oxidation,” *Chinese Journal of Catalysis*, vol. 39, pp. 630–638, 2018.
- [20] Y. Kim, J. Yoon, G.O. Park, S.B. Park, H. Kim, J.M. Kim and W.S. Yoon, “Enhancement of the interfacial reaction on mesoporous RuO<sub>2</sub> for next generation Li batteries,” *Journal of Power Sources*, vol. 396, pp. 749–753, 2018.
- [21] M. Taghizadeh, H. Akhoundzadeh and A. Rezayan, “Excellent catalytic performance of 3D-mesoporous KIT-6 supported Cu and Ce nanoparticles in methanol steam reforming,” *International Journal of Hydrogen Energy*, vol. 43, pp. 10926–10937, 2018.
- [22] S. Chirra, S. Siliveri, A. Kumar, A. Srinath, G. Sripal and R. Gujjula, “KIT-6: synthesis of a novel three-dimensional mesoporous catalyst and studies on its enhanced catalytic applications,” *Journal of Porous Materials*, vol. 26, pp. 1667–1677, 2019.
- [23] J.P. Ruelas-Leyva, A. Mata-Martinez, A. Talavera-López, S.A. Gómez, S.A. Jimenez-Lam and G.A. Fuentes, “Dehydrogenation of propane to propylene with highly stable catalysts of pt-sn supported over mesoporous silica KIT-6,” *International Journal of Chemical Reactor Engineering*, vol. 16, no. 10, pp. 1-9, 2018.
- [24] A. Mata-Martinez, S.A. Jimenez-Lam, A. Talavera-López, S.A. Gómez, G.A. Fuentes, L.A. Picos-Corrales, J.C. Piña-Victoria, J.P. Ruelas-Leyva, “The effect of Sn content in a Pt/KIT-6 catalyst over its performance in the dehydrogenation of propane,” *International Journal of Chemical Reactor Engineering*, vol. 16, no. 10, pp. 1-9, 2018.
- [25] H. Sun, C.M. Parlett, M.A. Isaacs, X. Liu, G. Adwek, J. Wang, B. Shen, J. Huang and J. Wu, “Development of Ca/KIT-6 adsorbents for high temperature CO<sub>2</sub> capture,” *Fuel*, vol. 235, pp. 1070-1076, 2019.
- [26] D. Xia, Y. Chen, C. Li, C. Liu and G. Zhou, “Carbon dioxide reforming of methane to syngas over ordered mesoporous Ni/KIT-6 catalysts,” *International Journal of Hydrogen Energy*, vol. 43, no. 45, pp. 20488-20499, 2018.
- [27] H. Liu, S. Xu, G. Zhou, K. Xiong, Z. Jiao, S. Wang, “CO<sub>2</sub> hydrogenation to methane over Co/KIT-6 catalysts: Effect of Co content,” *Fuel*, vol. 217, pp. 570-576, 2018.
- [28] J.M. Cho, G.Y. Han, H-K. Jeong, H-S. Roh and J.W. Bae, “Effects of ordered

- mesoporous bimodal structures of Fe/KIT-6 for CO hydrogenation activity to hydrocarbons,” *Chemical Engineering Journal*, vol. 354, pp. 197-207, 2018.
- [29] C. Tuncer, “Hydrothermal synthesis and sol-gel methods for CdS particle production in different morphologies and their use in wastewater applications,” *Sakarya University Journal of Science*, vol. 22, no. 3, pp. 888-897, 2018.
- [30] F.R.D. Fernandes, F.G.H.S. Pinto, E.L.F. Lima, L.D. Souza, V.P.S. Caldeira and A.G.D. Santos, “Influence of synthesis parameters in obtaining KIT-6 mesoporous material,” *Applied Sciences*, vol. 8, pp. 725-742, 2018.
- [31] M.M. Ayad, N.A. Salahuddin, A.A. El-nasr and N.L. Torad, “Amine-functionalized mesoporous silica KIT-6 as a controlled release drug delivery carrier,” *Microporous Mesoporous Materials*, vol. 229, pp. 166–177, 2016.
- [32] G.G. Karthikeyan, G. Boopathi and A. Pandurangan, “Facile synthesis of mesoporous carbon spheres using 3D cubic Fe-KIT-6 by CVD technique for the application of active electrode materials in supercapacitors,” *ACS Omega*, vol. 3, pp. 16658–16671, 2018.
- [33] R. Merkache, I. Fechete, M. Maamache, M. Bernard, P. Turek, K. Al-dalama and F. Garin, “3D ordered mesoporous Fe-KIT-6 catalysts for methylcyclopentane (MCP) conversion and carbon dioxide (CO<sub>2</sub>) hydrogenation for energy and environmental applications,” *Applied Catalysis A : General*, vol. 504, pp. 672–681, 2015.
- [34] J. Xu, Y. Hong, M.J. Cheng, B. Xue and Y.X. Li, “Vanadyl acetylacetonate grafted on ordered mesoporous silica KIT-6 and its enhanced catalytic performance for direct hydroxylation of benzene to phenol,” *Microporous and Mesoporous Materials*, vol. 285, pp. 223–230, 2019.
- [35] K.A. Cychosz and M. Thommes, “Progress in the physisorption characterization of nanoporous gas storage materials,” *Engineering*, vol. 4, pp. 559–566, 2018.
- [36] T.N. Phan, M.K. Gong, R. Thangavel, Y.S. Lee and C.H. Ko, “Enhanced electrochemical performance for EDLC using ordered mesoporous carbons (CMK-3 and CMK-8): Role of mesopores and mesopore structures,” *Journal of Alloys Compounds*, vol. 780, pp. 90–97, 2019.
- [37] R. Kishor and A.K. Ghoshal, “Understanding the hydrothermal, thermal, mechanical and hydrolytic stability of mesoporous KIT-6: A comprehensive study,” *Microporous and Mesoporous Materials*, vol. 242, pp. 127–135, 2017.
- [38] A. H. Elhaj Yousif, O. Y. Omer Alhussein and M. S. Ali Eltoun, “Characterization of hydrolyzed products of tetra ethoxy silane prepared by sol-gel method,” *International Journal of Multidisciplinary Sciences and Engineering*, vol. 6, pp. 19-24, 2015.
- [39] X. Shen, Y. Zhai, Y. Sun and H. Gu, “Preparation of monodisperse spherical SiO<sub>2</sub> by microwave hydrothermal method and kinetics of dehydrated hydroxyl,” *Journal of Material Science and Technology*, vol. 26, no. 8, pp. 711-714, 2010.